

Fabrication and mechanical properties of PLLA/PCL/HA composites via a biomimetic, dip coating, and hot compression procedure

L. F. Charles · M. T. Shaw · J. R. Olson ·
M. Wei

Received: 12 December 2009 / Accepted: 1 March 2010 / Published online: 18 March 2010
© Springer Science+Business Media, LLC 2010

Abstract Currently, the bone-repair biomaterials market is dominated by high modulus metals and their alloys. The problem of stress-shielding, which results from elastic modulus mismatch between these metallic materials and natural bone, has stimulated increasing research into the development of polymer-ceramic composite materials that can more closely match the modulus of bone. In this study, we prepared poly(L-lactic acid)/hydroxyapatite/poly(ϵ -caprolactone) (PLLA/HA/PCL) composites via a four-step process, which includes surface etching of the fiber, the deposition of the HA coating onto the PLLA fibers through immersion in simulated body fluid (SBF), PCL coating through a dip-coating process, and hot compression molding. The initial HA-coated PLLA fiber had a homogeneous and continuous coating with a gradient structure. The effects of HA: PCL ratio and molding temperature on flexural mechanical properties were studied and both were shown to be important to mechanical properties. Mechanical results showed that at low molding temperatures and up to an HA: PCL volume ratio of 1, the flexural strain decreased while the flexural modulus and strength increased. At higher mold temperatures with a lower viscosity of the PCL a HA: PCL ratio of 1.6 gave similar

properties. The process successfully produced composites with flexural moduli near the lower range of bone. Such composites may have clinical use for load bearing bone fixation.

1 Introduction

The majority of devices in use today for bone-repair (bone plates, pins, screws, etc.) are made from metal alloys. Metallic devices have high strength, modulus, and toughness, but are plagued with several deficiencies. The most frequently cited of these are stress-shielding tendencies, and the unpleasant retrieval surgery [1, 2]. Stress shielding arises from the large disparity in elastic modulus between metallic implants and natural bone. The elastic modulus of bone is typically within the range of 7–25 GPa depending on location, age, and the type of bone, with cortical bone being stiffer than trabecular bone [3–8]. For instance, the modulus of trabecular bone ranges from 1 to 14 GPa [6–13]. On the other hand, the elastic modulus of metals used in these applications ranges from 100 to 250 GPa [14]. Due to their significantly greater stiffness, the metallic implant sustains a greater portion of any load, and the stress-shielded bone may heal incompletely, which could lead to re-fracture [15]. In addition, there is also considerable interest in developing biodegradable replacements for metallic implants to eliminate the necessity to remove the implant after the bone has healed.

Human bone is a highly ordered and complex structure consisting mainly of inorganic apatite crystals and organic collagen fibers (mainly Type I) and carbonated apatite [16]. Due to its osteoconductive and biocompatible properties, hydroxyapatite is often a component of orthopedic devices. However, being a ceramic material, it is brittle, making it

L. F. Charles · M. Wei (✉)
Department of Chemical, Materials, and Biomolecular
Engineering, University of Connecticut, Storrs, CT 06269, USA
e-mail: m.wei@mail.ims.uconn.edu

M. T. Shaw
Polymer Program, Institute of Materials Science, University
of Connecticut, Storrs, CT 06269, USA

J. R. Olson
Teleflex Medical, 1295 Main Street, P. O. Box 219, Coventry,
CT 06238, USA

susceptible to cracking, which limits its use as a stand-alone material for bone-repair applications.

Synthetic, as well as some natural polymers are being studied as suitable materials for biomimicking the fibrous component in natural bone. There is a very short list of synthetic absorbable polymers that are components in medical device implants approved by the FDA. PLLA and poly(ϵ -caprolactone) (PCL) are both on that list. Poly(DL-lactic acid) was the earliest reported resorbable polymer to be used for fracture fixation [17]. Today, PLLA and its various copolymers are still subjects of ongoing research into the development of bioabsorbable orthopedic biomaterials, and are also among those that are already commercially available [18, 19].

Hydroxyapatite/polymer composites are a subject of interest to many researchers involved in bone-repair. Although addition of HA to PCL increases the modulus relative to that of pure PCL, the composite modulus is still very low, ranging from 1 to 3 GPa [20–24]. For example, PLA/HA bending modulus values of <1 GPa were reported by McManus et al. [25] using a four-point bending test. Bending moduli of 150, 250, 570 MPa were reported for conventional HA (particle size > 100 nm) at 30, 40, and 50 wt%, respectively. Shikinami et al. [26] studied the mechanical properties of hot-forged PLLA/HA (uncalcined, unsintered) composites. In their study, 20, 30, 40, and 50 wt% of HA were added to PLLA, and bending moduli ranging from 6.5 (20 wt%) to 12.3 GPa (50 wt%) were attained. Meanwhile, Russias et al. [27] reported up to 10 GPa for the modulus of a compression molded PLA/HA slurry composites containing calcined HA powders (50–90 wt%) and HA whiskers (70 and 80 wt%) measured by microindentation. Additionally, mechanical test results for HA/PLLA/PCL composites have been reported by Park et al. [28]. Their composites were prepared by melt-mixing the three components followed by hot pressing. The HA was fixed at 10 wt%, while the PCL amounts were set at 0, 5, 10, and 15 wt%, with the PLLA making up the difference. A maximum bending modulus of around 4 GPa and a bending strength of approximately 90 MPa were reported by a three-point bending test at 5 wt% PCL. More recently, Guarino and Ambrosio reported on the synergistic effect of PLA and calcium phosphate reinforcement of PCL composites [29]. The composites were prepared by first preparing a mix of PCL, sodium chloride, and α -tricalcium phosphate (α -TCP) at varying TCP/PCL volume ratios (0, 13, 20, and 26%). PLA fibers were then impregnated with the mixture by filament winding through the solution and the sodium chloride was subsequently leached out to generate porous PCL/TCP/PLA composites. A maximum compressive elastic modulus of 2.2 MPa was reported at 19 and 26 volume percent PLA and TCP, respectively.

In an attempt to improve the mechanical properties of HA/PLLA/PCL composites, our approach was to incorporate the PLLA as fiber reinforcement instead of as a melt or solvent cast matrix. Herein, we report on the mechanical properties of a composite system comprising HA-coated PLLA fibers in a PCL matrix. A biomimetic method was used to coat the fibers with HA, and a dip-coating procedure served for the application of PCL to the coated fiber. Compression molding at low temperatures was used to form the composites into a bar. The ratio of each component was manipulated so as to observe changes in mechanical properties based on composition. Our goal was to produce a fully biocompatible, bioactive, and bioabsorbable composite with adequate mechanical properties for load-bearing bone-repair applications.

2 Experimental procedures

2.1 Biomimetic apatite coating on PLLA fibers

Poly(L-lactic acid) (PLLA) yarn (120 filament, 540 denier) was supplied by Teleflex Medical, USA. Approximately 0.6 g of PLLA yarn was wrapped around an open PTFE frame (7.5 cm \times 4 cm \times 3 mm with an opening of 5.8 cm \times 2.8 cm \times 3 mm). Care was taken to avoid overlapping of the yarn on the frame. To determine the mass of the PLLA, each frame was weighed before and after wrapping with yarn. The PLLA fibers were etched using a 0.01 M calcium hydroxide solution for 1 h at 37°C. Upon removal, the samples were rinsed with DI water, dried in air for 24 h, and weighed.

A modified simulated body fluid (m-SBF) containing NaCl, NaHCO₃, MgCl₂·6H₂O, K₂HPO₄, CaCl₂, and HEPES (4-(2-hydroxyethyl)-1-piperazineethanesulfonic acid) was prepared using the method previously reported [30]. A comparison between the ion concentrations in m-SBF and blood plasma is given in Table 1.

Table 1 Ion concentrations in human blood plasma and m-SBF

Ion	Concentration (mM)	
	Blood Plasma	m-SBF
K ⁺	5.0	6.0
Na ⁺	142.0	109.5
Ca ²⁺	2.5	7.5
Mg ²⁺	1.5	1.5
Cl ⁻	103.0	110.0
HCO ₃ ⁻	27.0	17.5
SO ₄ ²⁻	0.5	0.0
HPO ₄ ²⁻	1.0	3.0

Calcium hydroxide etched fibers were immersed in 500 mL of m-SBF for 24 h at 42°C. At the end of the coating period, the frames were removed and the fibers were rinsed with DI water and left to dry for 24 h. After drying, the exposed surfaces of the frames were wiped clean of any deposits and weighed to determine the mass of the HA coating deposited on the fibers. This process was repeated up to six times by re-immersing samples into a fresh supply of m-SBF to increase the HA deposition.

2.2 PLLA/HA/PCL composite preparation

Preparation of the PLLA/HA/PCL composites involved several steps following the calcium hydroxide etching and SBF immersion. In the case of multiple immersion periods, the samples were rinsed, dried for 24 h, and the SBF solution was replaced. Following the SBF coating sequence, the frame with fibers was dip-coated into a solution of PCL ($M_n \sim 80$ kDa, Aldrich) dissolved in acetone at concentrations of 1, 2, and 5 g/dL. The samples were dried in air for 24 h, after which the exposed surfaces of the frames were wiped to remove any excess PCL. The initial weight of the frame was carefully recorded. After each step, (wrapping fibers onto the frame, SBF immersion, and PCL coating), the weight of the samples was recorded to determine the mass of PLLA fibers, HA, and PCL. After dip coating, the HA/PCL coated fibers were removed from the frame and placed into a custom-made aluminum slot mold (4 cm × 5 mm × 5 mm), and subjected to hot compression molding (Carver Laboratory Press, 2731, USA). The plates were heated to 85, 100, and 120°C and a thermocouple was used to measure the temperature of the mold. The samples were pressed under an average normal stress of 500 MPa for 30 min. Finally, the system was cooled to room temperature (while still under pressure) and the samples were removed from the mold. The dimensions of each sample were measured using a digital caliper.

3 Characterization

3.1 Contact angle measurement

To study the effect of surface etching on the water contact angle, PLLA films were prepared by dissolving PLLA fibers in chloroform (2 g/dL). The PLLA solution was then cast onto a clean, dry glass surface and left to air dry for 24 h. The resulting films were subsequently etched with calcium hydroxide under the conditions previously outlined for the fibers (0.01 M Ca(OH)₂, 37°C, 1 h). After drying, the hydrophilicity of the film was determined by measuring the water contact angle using a goniometer (Ramé-hart, 100-00 115, USA). This procedure is known as

the sessile drop technique. A 5- μ L drop of Milli-Q distilled water was dropped onto the surface of PLLA films at room temperature; the angle was measured after 20 s to allow the drop to settle. Three castings each were tested for both the etched and unetched groups. The average angle of six randomly placed drops was measured and recorded for each individual casting.

3.2 Rheometry

The effect of temperature on the viscosity of the PCL used in the experiments was studied using a controlled-strain rheometer (TA Instruments, ARES-LS, USA). Rheological tests were performed using a parallel plate fixture. Six PCL pellets were placed on the bottom plate was lowered so that it stood just above the pellets. The experiment was performed at a shear rate of 0.1 s⁻¹, and temperatures of 85, 100, and 120°C. The viscosity at each temperature was recorded.

3.3 Scanning electron microscopy

The surface morphology of the PLLA fibers before and after HA coating, and the cross-sections of the composites were observed using a field-emission scanning electron microscope (FESEM, JEOL JSM-6335F) and an environmental electron scanning microscope (ESEM, Philips ESEM 2020), respectively.

3.4 X-ray powder diffraction

An X-ray diffractometer (Bruker AXS D5005) was used to determine the crystallographic structure of the calcium phosphate (CaP) coating. The CaP crystals were isolated by dissolving the PLLA of the CaP-coated fibers in tetrahydrofuran (THF) and filtering. The residue was washed with ethanol three times, followed by DI water twice, and dried. Data was collected using a scan speed of 5.0°/min and a scan step of 0.02° through a 5–65° range. The obtained pattern was matched against standard patterns for calcium phosphates (JCPDS 09-0432).

3.5 Mechanical testing

A three-point bending jig was used to determine the flexural modulus, strength, and failure strain of the composites. The jig was mounted in an Instron tensile testing machine (Instron Instruments, 1011, UK) equipped with a 500-N load cell. A cross-head speed of 1 mm/min was used for all tests. The flexural stress and strain were calculated from the load and deflection data collected via the data acquisition system. The usual linear elastic formulas were used to calculate the maximum flexural stress (σ_f), modulus (E_f), and maximum strain (ϵ_f).

$$\sigma_f = \frac{3Fl}{2wt^2} E_f = \frac{l^3 m}{4wt^3} \varepsilon_f = \frac{6Dt}{l^2}$$

where F is the load, l is the support span, w is the width of the sample, t is the thickness the sample, D is the center deflection of the sample, and m is the slope of the initial straight-line portion of the force–deflection curve. Values are reported as mean \pm 95% confidence limit of the mean based on independently prepared test units, unless otherwise stated.

4 Results

4.1 Biomimetic coating on PLLA fibers

Prior to applying the biomimetic coating, the surface of the PLLA fiber was etched using calcium hydroxide solution. The goal was to increase hydrophilicity at the surface without appreciable mass loss. Water contact angles for unetched and etched PLLA films were $71.7 \pm 3.1^\circ$ and $63.3 \pm 2.1^\circ$, respectively. The decrease ($P < 0.05$) in contact angle suggests that hydrophilicity was improved at the surface following the etching procedure. Moreover, weight measurements before and after the etching showed no significant weight change.

The PLLA yarn was successively coated in modified SBF at 42°C . The mass of HA deposited after SBF immersion was found to increase linearly (Fig. 1) with number of immersions at a rate of ~ 5 wt% per immersion. It was found that, given the PCL solution concentrations used, up to six immersion cycles provided a maximum HA: PCL ratio while maintaining the intact and functionality of the composites. Figure 2a–d illustrates the homogeneity, thickness, and morphology of the HA layer after one SBF immersion cycle. The coating obtained was roughly $7\text{--}8 \mu\text{m}$ thick and appeared homogeneous and continuous along the fibers (Fig. 2b, c). The surface view suggested

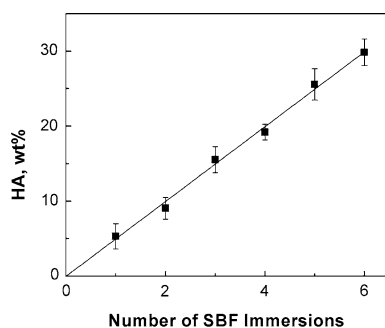


Fig. 1 Weight percent of HA deposited on PLLA fibers, based on original fiber mass, according to number of SBF immersions. Error bars represent 95% confidence limit of the mean of five independent determinations

that the coating comprised a porous network structure of plate-shaped apatite crystals (Fig. 2d). However, a cross-section view of the coating revealed that a gradient structure had formed with a dense layer on the bottom (closer to the fiber), and a porous layer at the surface (Fig. 3).

The XRD pattern of the coating recovered from the PLLA fibers is shown in Fig. 4. The pattern shows major peaks occurring around $2\theta = 26, 31\text{--}33, 40,$ and 53° , which coincide with those of the standard HA pattern, indicating that a pure HA coating had formed on the surface of the PLLA fibers. The XRD pattern (Fig. 4) also shows that the peaks in the $31\text{--}33^\circ$ range have merged into a single broad peak which could be influenced by small crystal size of the apatite.

4.2 Mechanical properties of composites

Typical stress–strain curves of the PLLA/HA/PCL composites investigated in this study using a three-point bend test are shown in Fig. 5. These curves correspond with those generally observed for ductile materials. Table 2 lists the compositional description of samples prepared for the study, along with sample IDs that will be used to refer to a particular sample. The mechanical properties of the composites prepared at a molding temperature of 85°C are given in Table 3.

The results showed a trend toward increase in modulus from 0/85 to 1/78 and a trend toward decrease in modulus from 1/78 to 2.7/89 as shown in Fig. 6a. Between HA: PCL ratio of 0 to 1, there is also a trend toward increase in σ_f (Fig. 6b); however, as with the modulus, we observed that beyond an HA: PCL ratio of 3 there was a trend toward decrease in σ_f .

Table 3 also shows the results of the flexural strain for composites where the molding temperature is 85°C . At this lower molding temperature it is observed that there is a trend toward decrease in ε_f (Fig. 6c) as the HA: PCL ratio increased, indicating the composite becomes more brittle with increasing HA loading. The low values of strain at break observed suggest very good adhesion of the PCL matrix to the PLLA fibers. Figure 7 shows the effect of increasing the molding temperature on the modulus between two composites with different HA: PCL ratios, and Table 4 presents the flexural strength data for the same set of samples. Two-way ANOVA, analyzing two different HA: PCL ratios (1 and 1.6) at three molding temperatures ($85, 100,$ and 120°C), was used to assess the effect of molding temperature and HA: PCL ratio on flexural modulus. The analysis revealed that there was a significant interaction between the two factors ($P < 0.05$). According to the data obtained, bending modulus increased when both molding temperature and HA: PCL composition were increased (Fig. 7). It is noteworthy, that at the higher mold

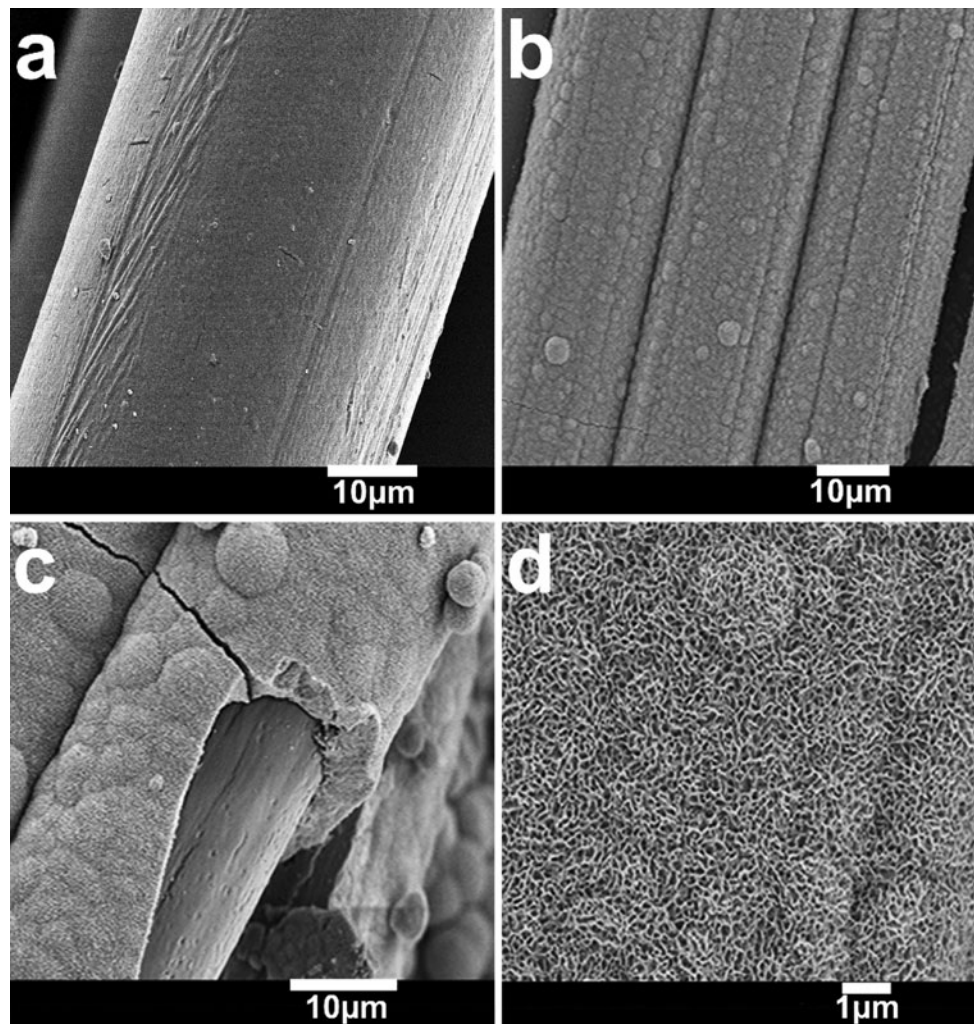


Fig. 2 FESEM images of apatite coating after one cycle of SBF immersion showing **a** the unetched, uncoated fiber, **b** the uniformity of the hydroxyapatite coating, **c** cross-section of the coating, and **d** the surface morphology of the apatite coating at a high magnification

temperatures the higher HA: PCL ratio produces better results.

5 Discussion

5.1 Biomimetic coating

Surface hydrolysis of polyesters by hydroxides is known to result in enhanced hydrophilicity, which suggests an increase in the concentration of carboxyl and hydroxyl groups on the polymer surface [31–34]. The hydroxide anions in the solution hydrolyze the ester groups on the surface of the PLLA fibers, which results in the breakage of the polymer chains and the formation of carboxyl and hydroxyl groups at the ends of the two new chains [35, 36]. The chemistry and mechanisms through which these reactions occur have been studied by others [37, 38].

Following this, the efficacy of the calcium hydroxide treatment to hydrolyze the PLLA was measured indirectly through water contact-angle measurement, which is commonly used in surface modification investigations [39–44]. There was a decrease ($P = 0.002$) in water contact angle of $8.4^\circ \pm 3.8^\circ$ after etching with $\text{Ca}(\text{OH})_2$, suggesting a more hydrophilic surface was achieved. This has been studied extensively because of the possibility that carboxylic acid groups generated from alkaline etching can promote the nucleation of CaP on different substrates [34, 45–49]. For example, Kawashita et al. [49] reported that calcium hydroxide can induce ester hydrolysis, leading to carboxylate groups, and this modification enhanced the apatite-forming ability on polymer gels. The HA deposition results obtained using this biomimetic coating method can be compared to other investigations of HA deposition on polymers via SBF [34, 49–52]. In a similar study involving deposition of HA on PLLA by immersing in 1.5 SBF [52],

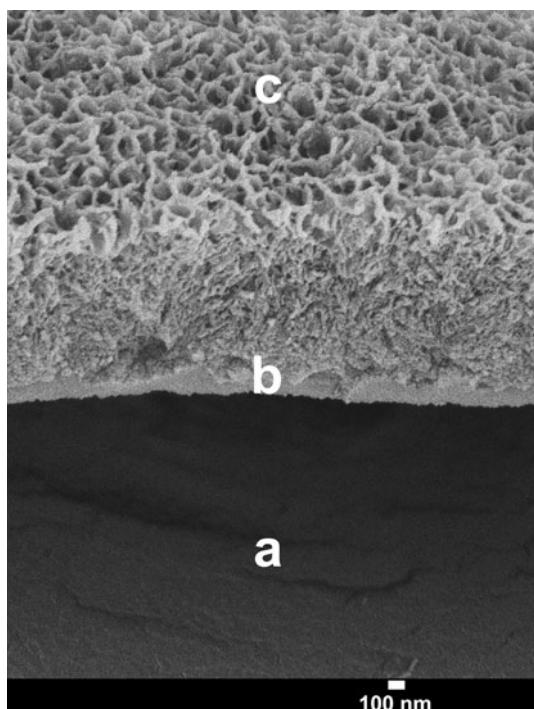


Fig. 3 FESEM image of gradient structure of biomimetic apatite coating deposited on the surface of a PLLA fiber showing dense inner layer with porous surface

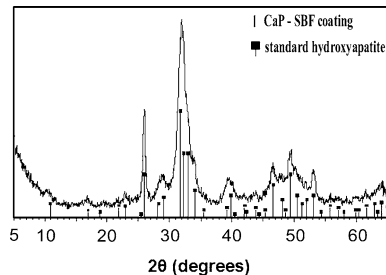


Fig. 4 XRD pattern of the apatite coating deposited on the PLLA fibers

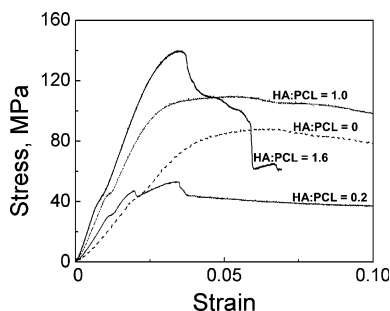


Fig. 5 Typical stress–strain curves for the different composites tested in this study at a molding temperature of 85°C. HA: PCL is given as volume ratio

Table 2 PLLA/HA/PCL volume percent compositions for samples (molding temperature = 85°C) presented in this study along with corresponding HA: PCL, and PLLA: PCL volume ratios

Sample ID	PLLA (%)	HA (%)	PCL (%)	HA: PCL (volume ratio)	PLLA: PCL (volume ratio)
0/85	85	0	15	0	5.7
0.2/83	83	3	14	0.2	6.0
0.4/80	80	6	14	0.4	5.7
0.6/92	92	3	5	0.6	18
1/78	78	11	11	1.0	7.1
1.3/75	75	14	11	1.3	6.8
1.6/87	87	8	5	1.6	17.4
2.5/86	86	10	4	2.5	21.5
2.7/89	89	8	3	2.7	29.7

Sample ID corresponds to HA: PCL volume ratio/PLLA volume %

Table 3 Mechanical properties of samples are detailed

Sample ID	Flexural modulus (GPa)	Flexural strength (MPa)	Flexural strain (%)
0/85	2.3 ± 0.2	89.0 ± 6.0	6.3 ± 0.2
0.2/83	4.6 ± 0.6	120.0 ± 6.0	4.6 ± 0.8
0.4/80	4.8 ± 0.5	110.0 ± 9.0	4.0 ± 0.8
0.6/92	5.1 ± 0.5	112.0 ± 23.0	3.1 ± 0.8
1/78	5.9 ± 1.0	129.0 ± 14.0	4.1 ± 0.9
1.3/75	5.4 ± 0.4	115.0 ± 15.0	3.3 ± 0.5
1.6/87	4.5 ± 0.7	71.0 ± 21.0	2.5 ± 0.2
2.5/86	3.9 ± 0.6	63.0 ± 15.0	3.0 ± 1.2
2.7/89	3.1 ± 0.3	50.0 ± 10.0	3.1 ± 1.1

Values reported are mean ± 95% confidence limit taken from five moldings. Molding temperature = 85°C

the authors reported a 40% mass increase after 30 days while others reported that up to 7 days was necessary to observe substantial coating on substrates [34, 49–51]. Meanwhile, we achieved a homogeneous and continuous coating layer after the first 24-h immersion cycle and a 30% mass increase of the PLLA fibers after six immersion cycles. The cross-sectional structure of the first coating layer exhibited a gradient that may be useful for loading of bioactive agents.

5.2 Mechanical properties of composites

Our results show the importance of having both the right amount of binding PCL matrix and the correct molding temperature to prepare optimum composites for bone-repair. We have found that as the HA: PCL ratio increases at lower molding temperatures, there is a trend in increase of the modulus of the composite, to a point (Fig. 6a). The

Fig. 6 Variation of composite **a** modulus, **b** strength, and **c** strain with matrix composition. The trend lines are empirical. The three parameters (y_0 , α , β) are significant for each curve. y_0 , α , β are **a** 2.4, 10.9, and 1.2, **b** 91.6, 201.8, and 0.9, **c** 3.1, 3.2, and 0.3, respectively

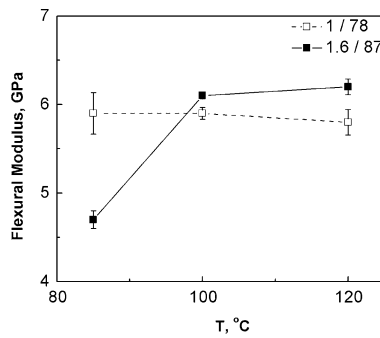
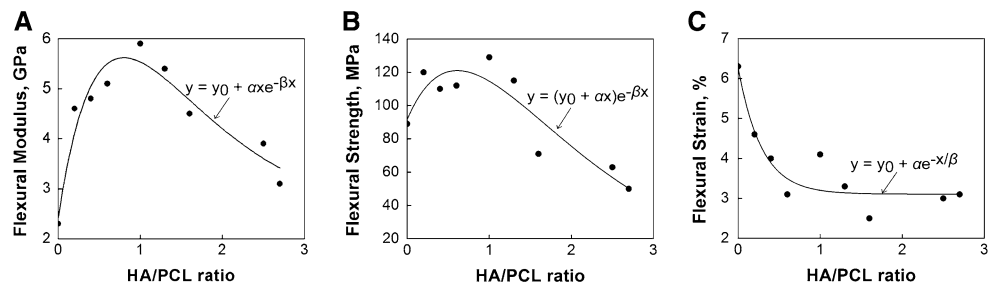


Fig. 7 Comparison of the elastic moduli of composites prepared with two different HA: PCL ratios (1 and 1.6) and molding temperatures of 85, 100, and 120°C. Error bars represent standard error of the mean of three moldings

Table 4 Comparison of composite flexural strength across different molding temperatures at two different HA: PCL ratios

Molding temperature (°C)	Flexural strength (MPa)	
	HA: PCL = 1	HA: PCL = 1.7
85	134 ± 1	71 ± 40
100	122 ± 38	125 ± 34
120	127 ± 22	132 ± 21

Values reported are mean ± 95% confidence limit taken from three moldings

Table 5 Inverse relationship between temperature and viscosity of the PCL used in this study (shear rate = 0.1 s⁻¹)

T (°C)	η (kPa s)
85	24
100	15
120	8

results obtained were higher than those presented in a similar PLLA/HA/PCL study by Park et al. [28]. However, while they have used melt-mixing to blend PLLA and PCL, our approach differed in that we incorporate PLLA as fiber reinforcement. In fibrous composites, unidirectional alignment of the fibers contributes significantly to improved

modulus and strength of the composites. Coupling this unidirectional alignment of the PLLA fibers with HA reinforcement contributes to the observed increase in flexural modulus. In addition, the toughness of the composite remains high.

To maximize the properties of the composite [53], it is important to minimize the amount of PCL in the composite, as the PCL has the lowest modulus and strength of the three components. On the other hand, if there is too little PCL there will not be sufficient matrix material to bond the fibers, and the high content of HA will decrease the toughness of the composite. At high HA: PCL ratios (1.6, 2.5, and 2.7), where we begin to observe a trend toward decrease in flexural strength, it is likely that there is insufficient PCL to bond the PLLA and HA together.

We hypothesized that increasing the temperature during the compression process would help to improve the mechanical properties of the composites. Results showed that in samples with a lower HA: PCL ratio (1.0), an increase in molding temperature did not significantly affect the flexural modulus. However, results observed for the samples with an HA: PCL ratio of 1.6 appeared consistent with the hypothesis (Fig. 7), which is supported by the significant synergistic relationship of HA: PCL ratio and molding temperature. This interaction suggests that increasing the molding temperature is helpful only if there is enough PCL to flow between the fibers.

The impact of molding temperature can be explained by the PCL temperature/viscosity relationship. Table 5 presents the results of the effect of increasing temperature on the viscosity of the PCL. As expected, the PCL viscosity decreases with increasing temperature. This is in accordance with results presented by others [54]. It was observed that increasing the temperature from 85 to 120°C decreased the viscosity threefold, thereby facilitating the flow of the molten PCL between the HA-coated fibers. The cross-sectional areas (Fig. 8) demonstrate the structural difference in samples prepared at two different HA: PCL ratios (1 and 1.6) and three different molding temperatures (85, 100, and 120°C).

Figure 8a–c shows composites with an HA: PCL ratio of 1.6 and pressed at temperatures of 85, 100, and 120°C, respectively. We observed that as the temperature was

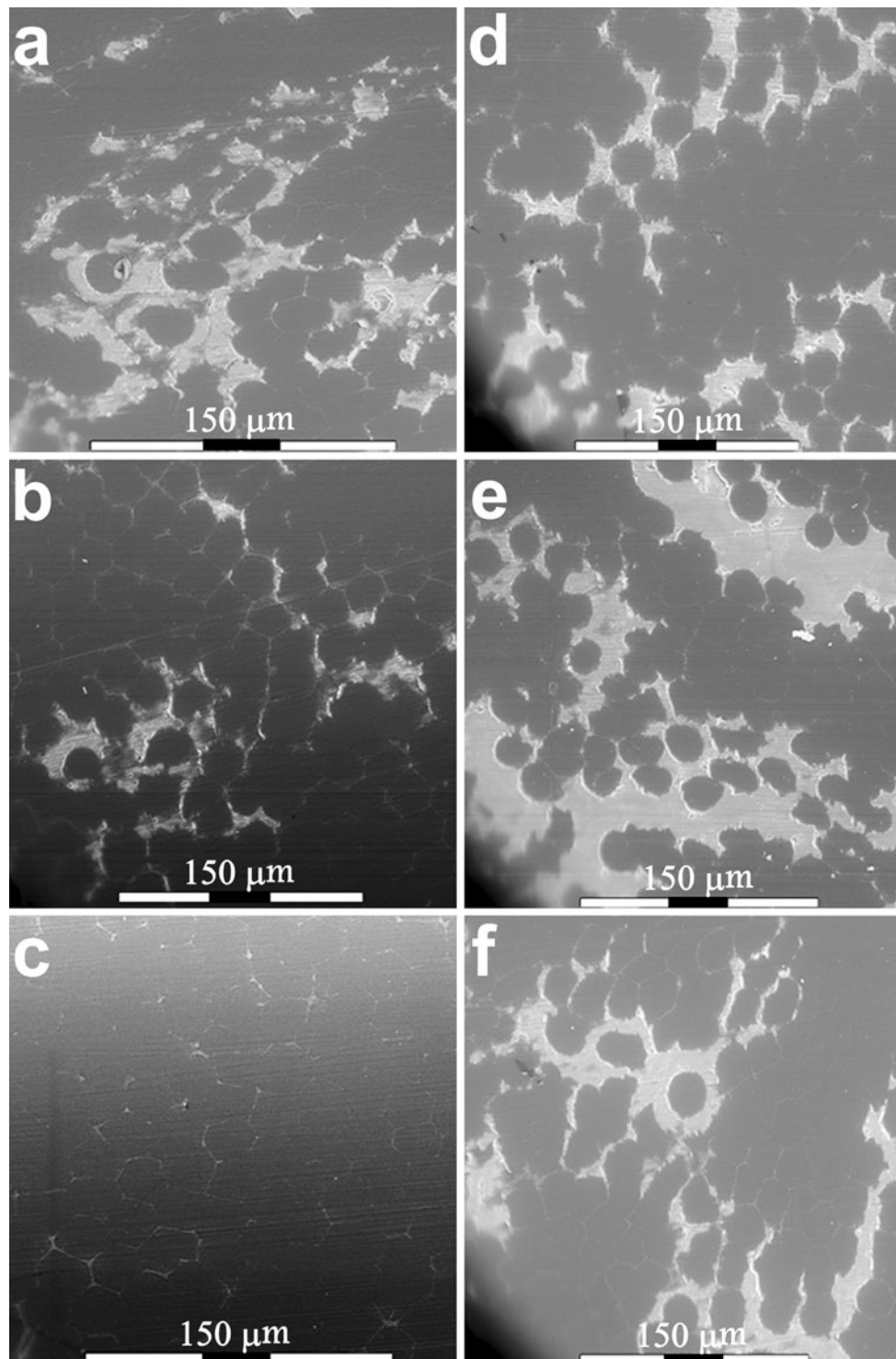


Fig. 8 Cross-sectional view of composites prepared at different HA: PCL ratios and molding temperatures (darker regions represent PLLA and lighter regions are PCL) as seen under ESEM. Images **a–c** were

prepared at HA: PCL = 1.6 and a molding temperature of 85, 100, and 120°C, respectively; images **d–f** were prepared at HA: PCL = 1 and a molding temperature of 85, 100, and 120°C, respectively

increased, the composites appear to become more compact, with fewer and smaller pockets of PCL in between the fiber clusters. Hence, the higher temperatures appear to lead to

better distribution of the PCL through the PLLA/HA structure. As the amount of HA increases and PCL decreases in the samples, it is possible that at 85°C the

relatively higher viscosity of the PCL (Table 5) and increasing amount of HA inhibits the ability of the polymer to effectively flow around and between the constituent fibers to create a strong bond. However, increasing the temperature, which dramatically lowers the viscosity, allows for the PCL to be better distributed around and between the fibers and create a well-bonded composite, which in conjunction with HA loading increases the modulus. This may account for the effect of molding temperature on the properties of samples with higher HA: PCL ratios. In contrast, at a low temperature (85°C) the increase in HA: PCL may introduce defects; which, in addition with the poor compression at this temperature, leads to reduced mechanical properties.

The appearance of the sections of the samples with an HA: PCL ratio of 1 (Fig. 8d–f), unlike that of the others (HA: PCL = 1.6), show no indication of significant detectable reduction in the PCL pockets between clusters of PLLA fibers or improved packing of the PLLA fibers even at elevated temperatures. This could mean that at an HA: PCL of 1, the composite may be over-saturated with PCL which prevents the fibers from becoming closely packed.

6 Conclusions

A four-step process consisting of surface etching, biomimetic coating, dip coating, and hot compression molding was implemented to produce PLLA/HA/PCL composites. Multiple immersions of calcium hydroxide etched PLLA fibers in m-SBF increased the deposition of HA. Composites prepared according to this process yielded flexural moduli in the range of 3.1–5.9 GPa compared to a control of 2.3 GPa at a molding temperature of 85°C. At low molding temperatures, mechanical testing revealed that as the HA: PCL ratio increased, flexural strain trended toward a decrease while flexural modulus showed a trend toward increase between HA: PCL ratio of 0 to 1 followed by a decrease as the HA: PCL was further increased. However, increasing molding temperature increased the modulus of the composites when the amount of PCL in the composite was sufficient to fill the interstices between the fibers. These results collectively demonstrate that manipulation of the HA: PCL ratio and molding temperature can lead to a range of composites with improved mechanical properties comparable to natural bone. Thus, the proposed processes may have potential to be used in fabricating load bearing bone fixtures in clinical applications.

Acknowledgments This manuscript is based upon work supported by NSF GOALI Grant BES-0503315, Connecticut Innovations under the Yankee Ingenuity Technology Competition and Teleflex Medical, Inc.

References

1. Cordewener FW, Schmitz JP. The future of biodegradable osteosyntheses. *Tissue Eng.* 2000;6(4):413–24.
2. Pietrzak WS. Principles of development and use of absorbable internal fixation. *Tissue Eng.* 2000;6(4):425–33.
3. Simkin A, Robin G. The mechanical testing of bone in bending. *J Biomech.* 1973;6(1):31–9.
4. Reilly DT, Burstein AH, Frankel VH. The elastic modulus for bone. *J Biomech.* 1974;7(3):271–5.
5. Rho JY, Kuhn-Spearing L, Zioupos P. Mechanical properties and the hierarchical structure of bone. *Med Eng Phys.* 1998;20(2): 92–102.
6. Zysset PK, Guo XE, Hoffler CE, Moore KE, Goldstein SA. Elastic modulus and hardness of cortical and trabecular bone lamellae measured by nanoindentation in the human femur. *J Biomech.* 1999;32(10):1005–12.
7. Ashman RB, Rho JY. Elastic modulus of trabecular bone material. *J Biomech.* 1988;21(3):177–81.
8. Choi K, Kuhn JL, Ciarelli MJ, Goldstein SA. The elastic moduli of human subchondral, trabecular, and cortical bone tissue and the size-dependency of cortical bone modulus. *J Biomech.* 1990;23(11):1103–13.
9. Kuhn JL, Goldstein SA, Choi K, London M, Feldkamp LA, Matthews LS. Comparison of the trabecular and cortical tissue moduli from human iliac crests. *J Orthop Res.* 1989;7(6):876–84.
10. Mente PL, Lewis JL. Experimental method for the measurement of the elastic modulus of trabecular bone tissue. *J Orthop Res.* 1989;7(3):456–61.
11. Rho JY, Ashman RB, Turner CH. Young's modulus of trabecular and cortical bone material: ultrasonic and microtensile measurements. *J Biomech.* 1993;26(2):111–9.
12. Ryan SD, Williams JL. Tensile testing of rodlike trabeculae excised from bovine femoral bone. *J Biomech.* 1989;22(4):351–5.
13. Goldstein SA. The mechanical properties of trabecular bone: dependence on anatomic location and function. *J Biomech.* 1987;20(11–12):1055–61.
14. Park JB, Bronzino JD. *Biomaterials: principles and applications.* Florida: CRC Press; 2000. p. 5.
15. Ramakrishna S, Huang Z-M, Kumar GV, Batchelor AW, Mayer J. *An introduction to biocomposites.* London: Imperial College Press; 2004. p. 191.
16. Weiner S, Wagner HD. The material bone: structure-mechanical function relations. *Annu Rev Mater Sci.* 1998;28(1):271–98.
17. Daniels AU, Chang MK, Andriano KP. Mechanical properties of biodegradable polymers and composites proposed for internal fixation of bone. *J Appl Biomater.* 1990;1(1):57–78.
18. Middleton JC, Tipton AJ. Synthetic biodegradable polymers as orthopedic devices. *Biomaterials.* 2000;21(23):2335–46.
19. Ambrose CG, Clanton TO. Bioabsorbable implants: review of clinical experience in orthopedic surgery. *Ann Biomed Eng.* 2004;32(1):171–7.
20. Chen B, Sun K. Mechanical and dynamic viscoelastic properties of hydroxyapatite reinforced poly(epsilon-caprolactone). *Polym Test.* 2005;24(8):978–82.
21. Sun JJ, Bae CJ, Koh YH, Kim HE, Kim HW. Fabrication of hydroxyapatite-poly(epsilon-caprolactone) scaffolds by a combination of the extrusion and bi-axial lamination processes. *J Mater Sci Mater Med.* 2007;18(6):1017–23.
22. Cerrai P, Guerra GD, Tricoli M, Krajewski A, Guicciardi S, Ravaglioli A, et al. New composites of hydroxyapatite and bioresorbable macromolecular material. *J Mater Sci Mater Med.* 1999;10(5):283–9.

23. Kim HW. Biomedical nanocomposites of hydroxyapatite/poly-caprolactone obtained by surfactant mediation. *J Biomed Mater Res.* 2007;83A(1):169–77.
24. Causa F, Netti PA, Ambrosio L, Ciapetti G, Baldini N, Pagani S, et al. Poly-epsilon-caprolactone/hydroxyapatite composites for bone regeneration: in vitro characterization and human osteoblast response. *J Biomed Mater Res.* 2006;76A(1):151–62.
25. McManus AJ, Doremus RH, Siegel RW, Bizios R. Evaluation of cytocompatibility and bending modulus of nanoceramic/polymer composites. *J Biomed Mater Res.* 2005;72A(1):98–106.
26. Shikinami Y, Okuno M. Bioresorbable devices made of forged composites of hydroxyapatite (HA) particles and poly-L-lactide (PLLA): part I. Basic characteristics. *Biomaterials.* 1999; 20(9):859–77.
27. Russias J, Saiz E, Nalla RK, Gryn K, Ritchie RO, Tomsia AP. Fabrication and mechanical properties of PLA/HA composites: a study of in vitro degradation. *Mater Sci Eng C Biomim Supramol Syst.* 2006;26(8):1289–95.
28. Park SD, Todo M, Arakawa K, Tsuji H, Takenoshita Y. Fracture properties of bioabsorbable HA/PLLA/PCL composite material. Singapore: SPIE; 2005. p. 838–843.
29. Guarino V, Ambrosio L. The synergistic effect of polylactide fiber and calcium phosphate particle reinforcement in poly epsilon-caprolactone-based composite scaffolds. *Acta Biomater.* 2008;4(6):1778–87.
30. Qu HB, Wei M. The effect of initial pH on morphology of biomimetic apatite coating. *Key Eng Mater.* 2007;330–332:757–60.
31. Iguer O, Demoustier-Champagne S, Marchand-Brynaert J, Daoust D, Sclavons M, Devaux J. Modification of polyolefin films surface with sodium hypochlorite. *J Appl Polym Sci.* 2006; 100(2):1184–97.
32. Cheng Z, Teoh SH. Surface modification of ultra thin poly (epsilon-caprolactone) films using acrylic acid and collagen. *Biomaterials.* 2004;25(11):1991–2001.
33. Murphy WL, Mooney DJ. Bioinspired growth of crystalline carbonate apatite on biodegradable polymer substrata. *J Am Chem Soc.* 2002;124(9):1910–7.
34. Tanahashi M, Yao T, Kokubo T, Minoda M, Miyamoto T, Nakamura T, et al. Apatite coating on organic polymers by a biomimetic process. *J Am Ceram Soc.* 1994;77(11):2805–8.
35. Flory PJ. Principles of polymer chemistry. New York: Cornell University Press; 1995. p. 85–91.
36. Gao J, Niklason L, Langer R. Surface hydrolysis of poly(glycolic acid) meshes increases the seeding density of vascular smooth muscle cells. *J Biomed Mater Res.* 1998;42A(3):417–24.
37. Miyazaki T, Ohtsuki C, Akioka Y, Tanihara M, Nakao J, Sakaguchi Y, et al. Apatite deposition on polyamide films containing carboxyl group in a biomimetic solution. *J Mater Sci Mater Med.* 2003;14(7):569–74.
38. Takeuchi A, Ohtsuki C, Miyazaki T, Tanaka H, Yamazaki M, Tanihara M. Deposition of bone-like apatite on silk fiber in a solution that mimics extracellular fluid. *J Biomed Mater Res.* 2003;65A(2):283–9.
39. Nie F-Q, Xu Z-K, Yang Q, Wu J, Wan L-S. Surface modification of poly(acrylonitrile-co-maleic acid) membranes by the immobilization of poly(ethylene glycol). *J Memb Sci.* 2004;235 (1–2):147–55.
40. Bae J-S, Seo E-J, Kang I-K. Synthesis and characterization of heparinized polyurethanes using plasma glow discharge. *Biomaterials.* 1999;20(6):529–37.
41. Luo W, Li S, Bei J, Wang S. Synthesis and characterization of poly(L-lactide)-poly(ethylene glycol) multiblock copolymers. *J Appl Polym Sci.* 2002;84(9):1729–36.
42. Inagaki N, Narushima K, Lim SK. Effects of aromatic groups in polymer chains on plasma surface modification. *J Appl Polym Sci.* 2003;89(1):96–103.
43. Inagaki N, Narushima K, Tsutsui Y, Ohyama Y. Surface modification and degradation of poly(lactic acid) films by Ar-plasma. *J Adhes Sci Technol.* 2002;16:1041–54.
44. Kang IK, Choi SH, Shin DS, Yoon SC. Surface modification of polyhydroxyalkanoate films and their interaction with human fibroblasts. *Int J Biol Macromol.* 2001;28(3):205–12.
45. Naka K, Chujo Y. Control of crystal nucleation and growth of calcium carbonate by synthetic substrates. *Chem Mater.* 2001; 13(10):3245–59.
46. Campbell AA, Fryxell GE, Linehan JC, Graff GL. Surface-induced mineralization: a new method for producing calcium phosphate coatings. *J Biomed Mater Res.* 1996;32A(1):111–8.
47. Tanahashi M, Matsuda T. Surface functional group dependence on apatite formation on self-assembled monolayers in a simulated body fluid. *J Biomed Mater Res.* 1997;34A(3):305–15.
48. Oyane A, Uchida M, Yokoyama Y, Choong C, Triffitt J, Ito A. Simple surface modification of poly(epsilon-caprolactone) to induce its apatite-forming ability. *J Biomed Mater Res.* 2005;75A(1):138–45.
49. Kawashita M, Nakao M, Minoda M, Kim HM, Beppu T, Miyamoto T, et al. Apatite-forming ability of carboxyl group-containing polymer gels in a simulated body fluid. *Biomaterials.* 2003;24(14):2477–84.
50. Kawai T, Ohtsuki C, Kamitakahara M, Miyazaki T, Tanihara M, Sakaguchi Y, et al. Coating of an apatite layer on polyamide films containing sulfonic groups by a biomimetic process. *Biomaterials.* 2004;25(19):4529–34.
51. Kim HM, Kishimoto K, Miyaji F, Kokubo T, Yao T, Suetsugu Y, et al. Composition and structure of apatite formed on organic polymer in simulated body fluid with a high content of carbonate ion. *J Mater Sci Mater Med.* 2000;11(7):421–6.
52. Zhang R, Ma PX. Porous poly(L-lactic acid)/apatite composites created by biomimetic process. *J Biomed Mater Res.* 1999;45A(4):285–93.
53. Nielsen LE, Landel RF. Mechanical properties of polymers and composites. New York: Marcel Dekker Inc; 1994. p. 398.
54. Sarazin P, Favis BD. Influence of temperature-induced coalescence effects on co-continuous morphology in poly([epsilon]-caprolactone)/polystyrene blends. *Polymer.* 2005;46(16):5966–78.